PERGAMON

International Journal of Solids and Structures 37 (2000) 969–990

INTERNATIONAL JOURNAL OF SOLIDS and STRUCTURES

www.elsevier.com/locate/ijsolstr

A contribution to the analysis of flexible link systems

Francesco Ubertini*

DISTART, Università degli Studi di Bologna, Viale Risorgimento 2, 40136 Bologna, Italy

Received 5 September 1997; in revised form 14 April 1998

Abstract

A numerical method of analysis for the inverse kinematics problem of flexible link systems is presented. The proposed method is based upon an iterative scheme, which consists of updating the system configuration stepwise, by correcting the positioning error due to link deformations through rigid body motions of finite amplitude. The resulting nonlinear compensation scheme reduces to the solution of the inverse and direct kinematics problems of a sequence of equivalent rigid link systems. These solutions are symbolically derived by means of the Gröbner basis method. The convergence analysis of the proposed algorithm is developed. The applicability and the performance of the present method are verified trough some numerical tests, highlighting its advantages and disadvantages in comparison with other methods found in the literature.

Keywords: Flexible link systems; Kinematics; Gröbner basis method; Nonlinear compensation scheme; Robotics

1. Introduction

The model of rigid links is extensively adopted for the kinematics analysis due to the massive structural design of industrial link systems (Fu et al., 1987; Koren, 1987; Paul, 1982). However, such a model results in a slight inaccuraccy in handling the kinematics problem of the new generation of link systems. In fact, to get high accuracy in motion controlling and to increase the operation speeds and payloads, they are more slender and lighter, thus more deformable, notwithstanding the employment of new materials such as composites.

The methods of analysis for the kinematics of link systems can be divided into numerical or local, and analytical or global methods. The first ones (Boudreau and Tukkan, 1996; Chang and Hamilton, 1991; Colbaugh et al., 1990; Derby, 1983; Lin et al., 1991; Svinin and Uchiyama, 1994; Tornambe, 1990), whose main feature is their general applicability, are often the only viable alternative for complex systems, such as the flexible ones. They are based upon some techniques or compensation schemes of a

* Fax: +39-051-2093495.
E-mail address: francesco.ubertini@mail.ing.unibo.it (F. Ubertini)

0020-7683/00/$ - see front matter
PII: S0020-7683(99)00106-7

linear type to correct the positioning error due to the link deformation. However, due to their nature, just one of the solutions of the problem is obtained and, in some cases, these methods present some delicate aspects regarding their convergence to the solution. On the other hand, the analytical methods (Baillieul and Martin, 1990; Canny, 1988; Cox et al., 1992; Gosselin et al., 1995; Innocenti, 1995; Lazard, 1992; Lazard and Merlet, 1994; Lopez and Recio, 1993; Lee and Liang, 1988; Mavroidis et al., 1994; Shahinpoor, 1992; Tsai and Morgan, 1985; Zhang and Song, 1992) are not always successfully applicable, since they require a heavy computational burden and are less effective when the complexity of the system to be analyzed increases. In spite of that, they are to be preferred if applicable, i.e. for the analysis of some undeformable (or rigid) link systems, since they offer all the symbolic solutions of the problem. The algebraic elimination methods, such as the Gröbner basis method (Cox et al., 1992; Lazard, 1992; Lopez and Recio, 1993) and Sylvester's dialytical elimination method (Mavroidis et al., 1994; Tsai and Morgan, 1985) have acquired a particular importance among the analytical procedures. At the current state of algorithmic developments (Char et al., 1991; Gräbe, 1993), the Gröbner basis method could be less effective with respect to the dialytical elimination method. However, it is the only analytical method which permits a systematic and a completely general approach to a problem without introducing extraneous solutions, as could occur when the dialytical elimination method is used.

A numerical method for the analysis of flexible link systems, based upon an iterative scheme, is presented in this paper. The method is applicable to any type of structure: serial, parallel or hybrid, whether kinematically undetermined (redundant) or not. The related algorithm consists of updating the system configuration stepwise, by correcting the positioning error due to the link deformation by means of rigid body motions of finite amplitude. The resulting compensation scheme is nonlinear and consists of solving the inverse and the direct kinematics problems of a sequence of equivalent rigid link systems. These solutions are symbolically derived using the Gröbner basis method, which is considered the most convenient approach in this context. The parametric solutions of the inverse and the direct problems are computed only once, in a preliminary phase and, thereafter, they are specialized at each iteration. Finally, the present nonlinear compensation scheme is more effective than the linear ones.

2. Governing equations and conventional approaches

Consider a system S, which is made up of flexible bodies (links) mutually connected by undeformable joints (Fig. 1). The terminal element of S, generally called the end-effector, is a special link which is used

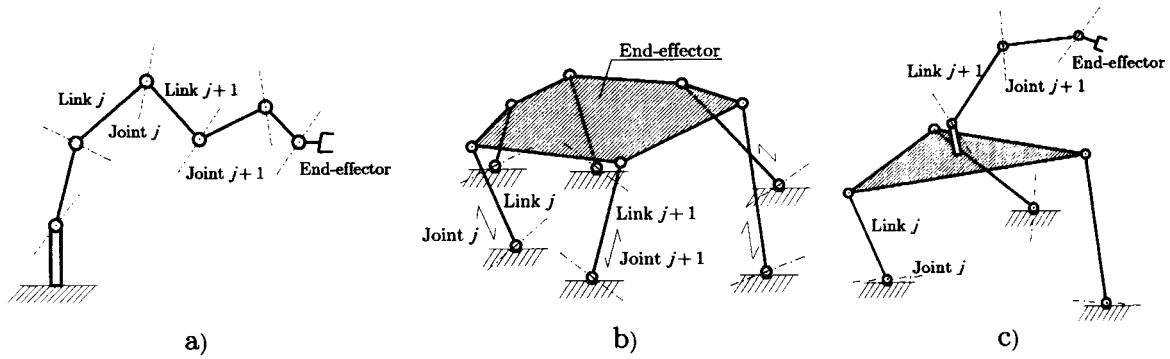

Fig. 1. Typologies of link systems: (a) serial, (b) parallel and (c) hybrid.

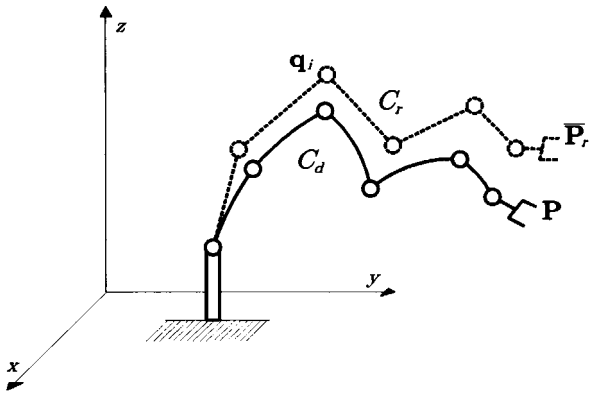

Fig. 2. The typical system configuration.

to interact with the environment and can be of various shapes (e.g. a grasping instrument, a platform, or other specific tools).

The typical configuration C of S can be represented by the superposition of the configuration C_r, which is obtained through relative joint movements by assuming the links as rigid bodies, and the configuration C_d, which derives from the previous one only through the deformation of the links (Chang and Hamilton, 1991; Fig. 2). The configuration C_r is described by the vector of the joint degrees of freedom, $\mathbf{q}$, by the end-effector position vector, $\mathbf{P}_r$, and by a vector of geometric parameters, $\mathbf{g}$, which describes the geometry of the links in their undeformed shape, according to a prescribed method of representation (e.g. Denavit and Hartenberg, 1955 for serial link systems).

Let n be the total number of the joint degrees of freedom in S, i.e. the dimension of $\mathbf{q}$, and J the set, of $\mathbb{R}^n$, of the possible values for $\mathbf{q}$:

$$\mathbf{q} \in J \subseteq \mathbb{R}^n.$$

Likewise, let m be the number of the independent parameters which identify the end-effector position, and W the set of $\mathbb{R}^m$ to which $\mathbf{P}_r$ belongs:

$$\mathbf{P}_r \in W \subseteq \mathbb{R}^m.$$

Sets J and W are referred to as the joint space and the workspace, respectively. If S is a redundant system, $n > m$, the joint degrees of freedom can always be distinguished in m dependent (or necessary) parameters and $n-m$ independent (or redundant) parameters. The latter ones, thought to be fixed, can be considered as formal geometric parameters and, consequently, included in $\mathbf{g}$. Thus, in the following, without loss of generality, n is assumed to be equal to m and therefore

$$\mathbf{q} \in J \subseteq \mathbb{R}^n$$

and

$$\mathbf{P}_r \in W \subseteq \mathbb{R}^n.$$

In the configuration C_r, the vector $\mathbf{P}_r$ is related to the vector $\mathbf{q}$ through the geometric parameters $\mathbf{g}$, by m compatibility equations (closure equations), which are generally strongly nonlinear. The system of these equations is represented synthetically as follows:

$$\mathbf{f}(\mathbf{q}, \mathbf{g}, \mathbf{P}_r) = \mathbf{0}. \tag{1}$$

The configuration C_d is determined by means of a displacement field defined on C_r. It can generally be computed as the solution of an elastic equilibrium problem defined on C_r and is related to the model employed for describing the deformative behavior of the links. Thus, the generalized displacement of the end-effector, due to the deformation of the links, is dependent on the configuration C_r:

$$\mathbf{u} = \mathbf{u}(\mathbf{q}, \mathbf{g}, \mathbf{P}_r).$$

It follows that the position $\mathbf{P}$ of the end-effector in the configuration C_d can be determined by the sum of the position $\mathbf{P}_r$, in C_r, and the vector $\mathbf{u}$:

$$\mathbf{P} = \mathbf{P}_r + \mathbf{u}(\mathbf{q}, \mathbf{g}, \mathbf{P}_r). \tag{2}$$

To sum up, the kinematics of a flexible link system is ruled by the system of $2n$ equations (Eqs. (1) and (2)):

$$\begin{cases} \mathbf{f}(\mathbf{q}, \mathbf{g}, \mathbf{P}_r) = \mathbf{0} \\ \mathbf{P} - \mathbf{P}_r - \mathbf{u}(\mathbf{q}, \mathbf{g}, \mathbf{P}_r) = \mathbf{0} \end{cases}. \tag{3}$$

When the system S has a serial structure, the configuration C_r is determined only by the couple $(\mathbf{q}, \mathbf{g})$, through the direct kinematic map $\mathbf{f}_s$, which relates the joint degrees of freedom to end-effector position. In this case, Eq. (3) can be rewritten in the simplified form

$$\begin{cases} \mathbf{P}_r + \mathbf{f}_s(\mathbf{q}, \mathbf{g}) = \mathbf{0} \\ \mathbf{P} - \mathbf{P}_r - \mathbf{u}(\mathbf{q}, \mathbf{g}) = \mathbf{0} \end{cases}. \tag{4}$$

On the other hand, when the system S has a parallel structure, C_r is determined only by the couple $(\mathbf{g}, \mathbf{P}_r)$, through the inverse kinematic map $\mathbf{f}_p$, and Eq. (3) reduces to the uncoupled system

$$\begin{cases} \mathbf{q} + \mathbf{f}_p(\mathbf{g}, \mathbf{P}_r) = \mathbf{0} \\ \mathbf{P} - \mathbf{P}_r - \mathbf{u}(\mathbf{g}, \mathbf{P}_r) = \mathbf{0} \end{cases}. \tag{5}$$

The direct kinematics problem consists of solving Eq. (3) for the $2n$ unknowns, $\mathbf{P}$ and $\mathbf{P}_r$, i.e. in determining all the end-effector positions $\mathbf{P}$, if they exist, compatible with a given value, $\bar{\mathbf{q}} \in J$, of the joint degrees of freedom. This problem can be solved by firstly determining all the configurations C_r which are compatible with $\bar{\mathbf{q}}$ and, subsequently, by computing for each of them the displacement of the end-effector, $\mathbf{u}$. The inverse kinematics problem, the dual of the previous one, consists of solving Eq. (3) for the $2n$ unknowns, $\mathbf{P}_r$ and $\mathbf{q}$, i.e. in determining all the vectors $\mathbf{q}$, if they exist, which are compatible with a given end-effector position $\bar{\mathbf{P}} \in W$. The inverse kinematics problem is generally more complex than the direct one, since the configuration C_r, on which C_d depends, is unknown. In the following, the interest is focused on the solution of the inverse problem and the features of the usually employed numerical methods are discussed.

The governing equations Eq. (3), making use of a compact notation, can be rewritten as

$$\mathbf{F}(\mathbf{x}) = \mathbf{0}, \tag{6}$$

where

$$\mathbf{x} = \begin{bmatrix} \mathbf{q} \\ \mathbf{P}_r \end{bmatrix}$$

and

$$\mathbf{F}(\mathbf{q}, \mathbf{P}_r) = \begin{bmatrix} \mathbf{f}(\mathbf{q}, \mathbf{P}_r) \\ \mathbf{P}_r + \mathbf{u}(\mathbf{q}, \mathbf{P}_r) - \bar{\mathbf{P}} \end{bmatrix}.$$

All the methods presented are based upon an iterative scheme, which can generally be written in the form

$$\mathbf{x}^{(k+1)} = \mathbf{x}^{(k)} - \mathbf{A}^{-1}\mathbf{F}(\mathbf{x}^{(k)}). \tag{7}$$

Subscripts taken in parentheses denote the iteration number, $\mathbf{x}^{(k)}$ is the value of vector $\mathbf{x}$ at the k-th step and $\mathbf{A}$ is a non singular $2n \times 2n$ matrix, which is called the iteration matrix and which can or cannot be dependent on $\mathbf{x}$.

At each step, the difference between the current approximation and the solution $\bar{\mathbf{x}}$ is called the error vector and is denoted by $\mathbf{e}^{(k)}$,

$$\mathbf{e}^{(k)} = \mathbf{x}^{(k)} - \bar{\mathbf{x}}.$$

2.1. Newton–Raphson method

The most popular, and general, approach to solve a system of nonlinear equations is the Newton–Raphson method, which derives from Eq. (7) by taking

$$\mathbf{A}(\mathbf{x}) = \mathbf{F}'(\mathbf{x}),$$

where $\mathbf{F}'(\mathbf{x})$ is the Gateaux derivative of $\mathbf{F}$ at $\mathbf{x}$,

$$\mathbf{F}'(\mathbf{x}) = \begin{bmatrix} \mathbf{J}_q(\mathbf{x}) & \mathbf{J}_P(\mathbf{x}) \\ \mathbf{U}_q(\mathbf{x}) & \mathbf{I} + \mathbf{U}_P(\mathbf{x}) \end{bmatrix}$$

and

$$\mathbf{J}_q = \frac{\partial \mathbf{f}}{\partial \mathbf{q}},$$

$$\mathbf{J}_P = \frac{\partial \mathbf{f}}{\partial \mathbf{P}_r},$$

$$\mathbf{U}_q = \frac{\partial \mathbf{u}}{\partial \mathbf{q}}$$

and

$$\mathbf{U}_P = \frac{\partial \mathbf{u}}{\partial \mathbf{P}_r}.$$

The method is locally convergent and exhibits a quadratic rate of convergence.

The main drawback of this scheme lies in the computation of its iteration matrix, which is an extremely huge and cumbersome task since the matrices, $\mathbf{U}_q$ and $\mathbf{U}_P$, are dependent not only on the geometrical properties of S but also on the model employed to describe its deformative behavior. Such a dependence implies an *ad hoc* implementation of the algorithm for each choice of the deformative

model. Moreover, the method is not always applicable, since $\mathbf{F}'(\mathbf{x})$ can be singular and it is very complex to calculate its points of singularity.

In spite of its good convergence properties, all this makes the Newton–Raphson method inapplicable in practice, except for link systems of very simple structure (Lin et al., 1991).

2.2. Linear compensation schemes

To overcome the disadvantages of the Newton–Raphson method, some algorithms based on linear compensation schemes have been proposed in the literature.

2.2.1. Linear compensation of the joint degrees of freedom (Lin et al., 1991) — RLC method

The method proposed in Lin et al. (1991) for the kinematics analysis of serial link systems is here outlined by extending it to hybrid ones. It is called the *RLC* method in the following.

The iterative algorithm is derived from Eq. (7) by taking

$$\mathbf{A}(\mathbf{x}) = \mathbf{A}_{\mathrm{LC}}(\mathbf{x}),$$

where

$$\mathbf{A}_{\mathrm{LC}}(\mathbf{x}) = \begin{bmatrix} \mathbf{J}_q(\mathbf{x}) & \mathbf{J}_P(\mathbf{x}) \\ \mathbf{0} & \mathbf{I} \end{bmatrix}. \tag{8}$$

This scheme is based upon the idea of correcting the positioning error stepwise, only through relative joint movements of small amplitude. As it can be seen by substituting Eq. (8) in Eq. (7), the small corrections are computed by solving for $\mathbf{q}$ the compatibility equations linearized in the neighborhood of the current rigid configuration $C_{\mathrm{r}}^{(k)}$:

$$\mathbf{J}_q^{(k)}(\mathbf{q} - \mathbf{q}^{(k)}) + \mathbf{J}_P^{(k)}\left(\mathbf{P}_{\mathrm{r}} - \mathbf{P}_{\mathrm{r}}^{(k)}\right) = \mathbf{0}.$$

Decomposing $\mathbf{F}'(\mathbf{x})$ as

$$\mathbf{F}'(\mathbf{x}) = \mathbf{A}_{\mathrm{LC}}(\mathbf{x}) + \mathbf{U}(\mathbf{x})$$

with

$$\mathbf{U}(\mathbf{x}) = \begin{bmatrix} \mathbf{0} & \mathbf{0} \\ \mathbf{U}_q(\mathbf{x}) & \mathbf{U}_P(\mathbf{x}) \end{bmatrix},$$

the convergence condition of the algorithm (Ortega and Rheinboldt, 1970) is given by

$$\rho\left(\mathbf{A}_{\mathrm{LC}}^{-1}(\bar{\mathbf{x}})\mathbf{U}(\bar{\mathbf{x}})\right) \ll 1, \tag{9}$$

where ρ denotes the matrix spectral radius.

Therefore the *RLC* algorithm is locally convergent to $\bar{\mathbf{x}}$ if the derivatives of the displacement with respect to $\mathbf{q}$ and $\mathbf{P}_{\mathrm{r}}$ are sufficiently small for admitting

$$\rho(\mathbf{U}(\bar{\mathbf{x}})) < 1.$$

Moreover, it can be seen that this scheme exhibits a linear rate of convergence.

The outlined method overcomes some drawbacks of the Newton–Raphson scheme. The iteration matrix Eq. (8) is dependent only on the geometric features of S, so that it is not related to the

deformative model employed or to the displacement field. However, the method is applicable only when the matrix $\mathbf{A}_{\mathrm{LC}}$ is non-singular so that the inverse exists

$$\mathbf{A}_{\mathrm{LC}}^{-1}(\mathbf{x}) = \begin{bmatrix} \mathbf{J}_q^{-1}(\mathbf{x}) & \mathbf{J}_q^{-1}(\mathbf{x})\mathbf{J}_P(\mathbf{x}) \\ \mathbf{0} & \mathbf{I} \end{bmatrix}. \tag{10}$$

From Eq. (10), $\mathbf{A}_{\mathrm{LC}}$ is non-singular if and only if $\mathbf{J}_q$ is non-singular. Couples $(\mathbf{q}, \mathbf{P}_{\mathrm{r}})$, describing configurations C_{r} in which $\mathbf{J}_q$ is singular, are called kinematic singularities of S. As a consequence, the algorithm does not converge close to the kinematic singularities. In order to avoid this disadvantage, it is necessary to map in advance such singularities in order to confine the applicability of the method.

Another drawback of the *RLC* scheme lies in the necessity of a starting point sufficiently accurate to guarantee the convergence to the solution. Therefore, if a good initial configuration is not known, the method needs to be started up. Finally, only one solution of the problem can be obtained.

2.2.2. Linear compensation of the relative elastic deflection (Svinin and Uchiyama, 1994) — DLC method

An iterative algorithm based upon a linear compensation scheme of the relative elastic deflections has been proposed in Svinin and Uchiyama (1994). The method has been developed only for serial link systems and consists of compensating stepwise for the difference between the previous and the current deflections. From here onwards, it will be referred to as the *DLC* method.

The initial configuration is set as

$$\begin{cases} \mathbf{q}^{(0)} = \mathbf{q}_{\mathrm{r}} \\ \mathbf{P}^{(0)} = \bar{\mathbf{P}} \end{cases},$$

where $\mathbf{q}_{\mathrm{r}}$ and $\bar{\mathbf{P}}$ simultaneously satisfy the compatibility equations.

Taking the compensation condition as

$$\Delta\mathbf{P} = \mathbf{P}^{(k+1)} - \mathbf{P}^{(k)} = \mathbf{0},$$

and linearizing the compatibility equations, written for serial link systems, in the neighborhood of $C_{\mathrm{r}}^{(k)}$, it follows that

$$\mathbf{J}_q^{(k)}(\mathbf{q} - \mathbf{q}^{(k)}) + (\mathbf{u} - \mathbf{u}^{(k)}) = \mathbf{0}.$$

Thereby, the iterative scheme reads as

$$\begin{cases} \mathbf{q}^{(k+1)} = \mathbf{q}^{(k)} - \mathbf{J}_q^{(k)-1}(\mathbf{u}^{(k)} - \mathbf{u}^{(k-1)}) \\ \mathbf{P}_{\mathrm{r}}^{(k+1)} = -\mathbf{f}_S(\mathbf{q}^{(k+1)}) \end{cases}.$$

Under the assumptions shown in Svinin and Uchiyama (1994), the algorithm converges to the couple $(\hat{\mathbf{q}}, \hat{\mathbf{P}}_{\mathrm{r}})$ but, in general, it can be shown that

$$\hat{\mathbf{P}} \neq \bar{\mathbf{P}},$$

where $\hat{\mathbf{P}}$ is the final end-effector position:

$$\hat{\mathbf{P}} = \hat{\mathbf{P}}_{\mathrm{r}} + \mathbf{u}(\hat{\mathbf{q}}).$$

It follows that the algorithm does not generally converge to a solution of Eq. (4) and, furthermore, it needs to be started up by computing a solution of Eq. (1) compatible with the target position.

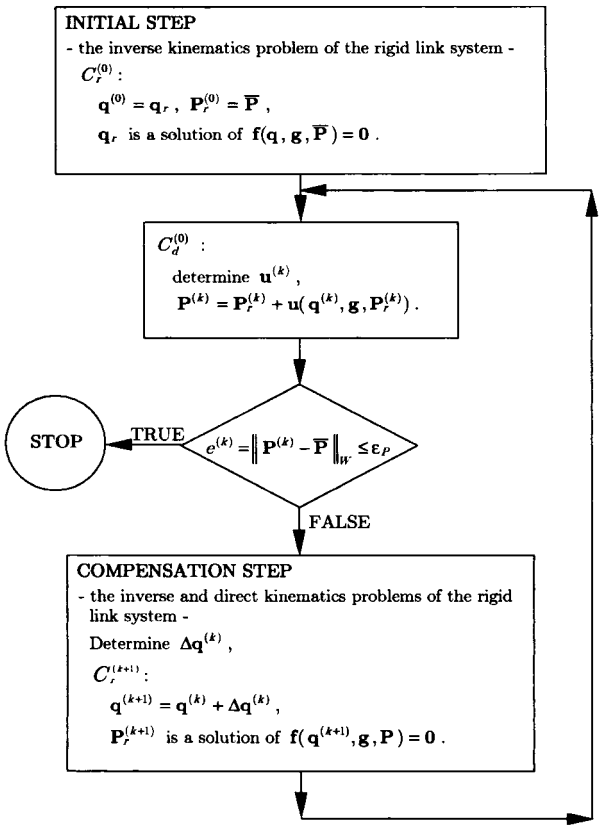

Fig. 3. Flow chart of the proposed algorithm.

3. The proposed algorithm

The proposed algorithm for the inverse kinematics analysis of S is based upon an iterative scheme (Fig. 3) and consists of updating stepwise the configuration of S only by means of rigid body motion corrections (Ubertini, 1996).

The initial configuration of S is defined by assuming a rigid link configuration, $C_{\mathrm{r}}^{(0)}$, which is compatible with $\bar{\mathbf{P}}$, and by determining the vector $\mathbf{u}$, i.e. the deformed configuration $C_{\mathrm{d}}^{(0)}$ referred to $C_{\mathrm{r}}^{(0)}$ [Fig. 4(a)]. The end-effector position vector $\mathbf{P}^{(0)}$, in the configuration $C_{\mathrm{d}}^{(0)}$, is generally different from $\bar{\mathbf{P}}$ because of the displacement due to the link deformation. The distance

$$e^{(k)} = \|\bar{\mathbf{P}} - \mathbf{P}^{(k)}\|_W,$$

between the end-effector position vector $\mathbf{P}^{(k)}$ in $C_{\mathrm{d}}^{(k)}$ and the target position $\bar{\mathbf{P}}$, is referred to as the end-effector positioning error — symbol $\|.\|_W$ denotes the assumed (euclidean) norm in W.

At each iteration, the end-effector positioning error is corrected through the compensation step described in the following section. It consists of updating the actual rigid configuration $C_{\mathrm{r}}^{(k)}$ by means of suitable finite adjustments of the joint degrees of freedom [Fig. 4(b,c)].

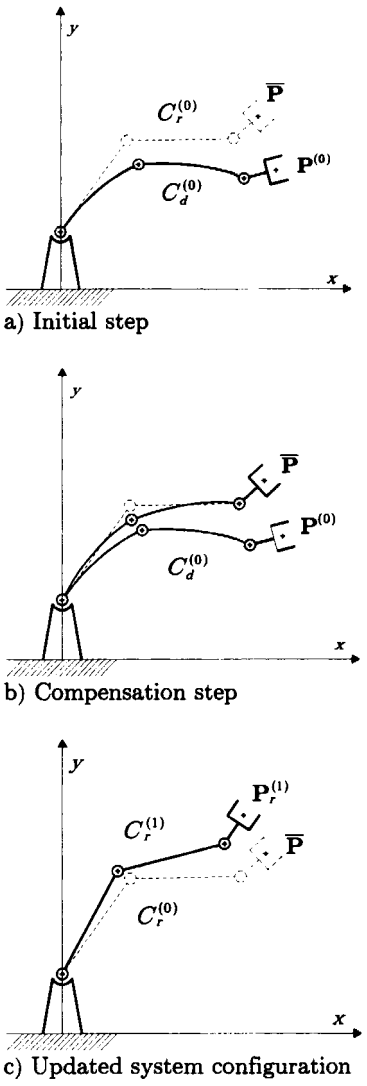

Fig. 4. First step.

The proposed iterative scheme develops as follows.

- Initial step.
  The configuration $C_{\mathrm{r}}^{(0)}$ is defined by setting:

$$\mathbf{q}^{(0)} = \mathbf{q}_{\mathrm{r}}$$

and

$$\mathbf{P}_{\mathrm{r}}^{(0)} = \bar{\mathbf{P}},$$

where $\mathbf{q}_{\mathrm{r}}$ is a solution of the inverse kinematics problem of the rigid link system

$$\mathbf{f}(\mathbf{q}, \mathbf{g}, \bar{\mathbf{P}}) = \mathbf{0}. \tag{11}$$

- k-th step.
  - The configuration $C_{\mathrm{d}}^{(k)}$, relative to $C_{\mathrm{r}}^{(k)}$, and the correspondent end-effector position

    $$\mathbf{P}^{(k)} = \mathbf{P}_{\mathrm{r}}^{(k)} + \mathbf{u}\left(\mathbf{q}^{(k)}, \mathbf{g}, \mathbf{P}_{\mathrm{r}}^{(k)}\right)$$

    are determined,
  - if the end-effector positioning error, $e^{(k)}$, is smaller than a prescribed tolerance ε_{p}:

    $$e^{(k)} = \|\bar{\mathbf{P}} - \mathbf{P}^{(k)}\|_W \leq \varepsilon_{\mathrm{p}},$$

    the procedure terminates. Otherwise:

- k-th compensation step.
  - The rigid body motion correction, $\Delta\mathbf{q}^{(k)}$, is determined (the details are given in Section 5),
  - the configuration $C_{\mathrm{r}}^{(k+1)}$ is defined by setting

    $$\mathbf{q}^{(k+1)} = \mathbf{q}^{(k)} + \Delta\mathbf{q}^{(k)},$$

    and by computing the resulting end-effector position, $\mathbf{P}_{\mathrm{r}}^{(k+1)}$, through the resolution of the direct kinematics problem of the rigid link system

    $$\mathbf{f}(\mathbf{q}^{(k+1)}, \mathbf{g}, \mathbf{P}) = \mathbf{0}. \tag{12}$$

The outlined algorithm, repeated for each solution of Eq. (11) taken as the initial configuration C_{r}, allows us to obtain all the solutions of the considered problem (3).

4. The compensation scheme

The compensation scheme consists of updating the rigid configuration of S, at the typical step k, through the rigid body motion resulting from a suitable finite increment, $\Delta\mathbf{q}^{(k)}$, of relative joint movements. Therefore, the compensation scheme is composed of two distinct phases: the computation of the finite increment $\Delta\mathbf{q}^{(k)}$ and the definition of the rigid configuration $C_{\mathrm{r}}^{(k+1)}$.

The configuration $C_{\mathrm{d}}^{(k)}$ can be equivalently represented either as the deformed configuration of S or as the configuration assumed by a hypothetical rigid link system, $S_{\mathrm{r}}^{(k)}$. Thereby $C_{\mathrm{d}}^{(k)}$, considered as a configuration of $S_{\mathrm{r}}^{(k)}$, is described by a vector of joint degrees of freedom, $\mathbf{q}_{\mathrm{d}}^{(k)}$, by the actual end-effector position $\mathbf{P}^{(k)}$ and by a vector, $\mathbf{g}_{\mathrm{d}}^{(k)}$, which describes the geometry of the elements of $S_{\mathrm{r}}^{(k)}$ (Fig. 5). As for the vector $\mathbf{g}$, the geometrical parameters collected in $\mathbf{g}_{\mathrm{d}}^{(k)}$ are evaluated according to the adopted method of geometry representation (e.g. Denavit and Hartenberg, 1955 for serial link systems). The idea of the hypothetical rigid link system was first proposed by Derby (1983) in the context of serial link systems and more details about the evaluation of $\mathbf{q}_{\mathrm{d}}^{(k)}$ and $\mathbf{g}_{\mathrm{d}}^{(k)}$ can be found in his work. However, it is worthy of note that these vectors are to be computed at each step, since $S_{\mathrm{r}}^{(k)}$ depends on the actual deformed configuration $C_{\mathrm{d}}^{(k)}$.

Once the vectors $\mathbf{q}_{\mathrm{d}}^{(k)}$ and $\mathbf{g}_{\mathrm{d}}^{(k)}$ are determined, the configuration of $S_{\mathrm{r}}^{(k)}$ they describe is updated by leading the end-effector from the actual position $\mathbf{P}^{(k)}$ to the target position (Fig. 5). This is equivalent to solving the inverse kinematics problem of $S_{\mathrm{r}}^{(k)}$:

$$\mathbf{f}\left(\mathbf{q}, \mathbf{g}_{\mathrm{d}}^{(k)}, \bar{\mathbf{P}}\right) = \mathbf{0}. \tag{13}$$

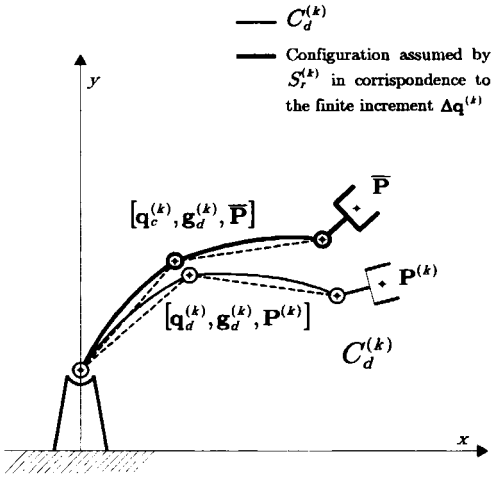

Fig. 5. Compensation step.

Eq. (13) is nonlinear and generally admits, except for parallel link systems, more than one solution (Mavroidis et al., 1994). Let $\mathbf{q}_c^{(k)}$ be the solution of Eq. (13) such that the quantity

$$\|\mathbf{q}^{(0)} - \mathbf{q}_{ci}^{(k)}\|_J \tag{14}$$

takes minimum over the set of the possible solutions of Eq. (13), $\mathbf{q}_{ci}^{(k)}$ — symbol $\|.\|_J$ denotes the assumed (euclidean) norm in J. Then the relative joint movements correction is given by

$$\Delta\mathbf{q}^{(k)} = \mathbf{q}_c^{(k)} - \mathbf{q}_{\mathrm{d}}^{(k)}.$$

Now, the configuration $C_{\mathrm{r}}^{(k+1)}$ is completely determined by computing $\mathbf{P}_{\mathrm{r}}^{(k+1)}$. In order to do that, the direct kinematics problem (12) needs to be solved. The system of Eq. (12) is nonlinear too, and generally admits, except for serial link systems, more than one solution (Lazard, 1992). Thus, assuming $C_{\mathrm{r}}^{(k+1)}$ as the configuration whose end-effector position is the closest one to $\bar{\mathbf{P}}$, $\mathbf{P}_{\mathrm{r}}^{(k+1)}$ is the solution of Eq. (12) such that the quantity

$$\|\bar{\mathbf{P}} - \mathbf{P}_{\mathrm{r}i}^{(k+1)}\|_W \tag{15}$$

takes minimum over the set of the feasible solutions of Eq. (15), $\mathbf{P}_{\mathrm{r}i}^{(k+1)}$.

Eq. (14) or Eq. (15) could become ineffective if two or more solutions of Eq. (12) belong to a ball of J with the center in $\mathbf{q}^{(0)}$ and sufficiently small radius, or else if two or more end-effector positions compatible with $\mathbf{q}^{(0)}$ belong to a ball of W with the center in $\bar{\mathbf{P}}$ and sufficiently small radius. However, in these cases, an *a posteriori* criterion can be adopted instead of Eqs. (14) and (15). It consists of assuming $C_{\mathrm{r}}^{(k+1)}$ as the configuration which is affected by the least positioning error among all the possible configurations compatible with the solutions of Eq. (13) and the related solutions of Eq. (12).

To sum up, the present compensation scheme reduces at each step to the solution of an inverse and a direct kinematics problem of rigid link systems. The solutions are here derived in symbolic form using the Gröbner basis method (Buchberger, 1985; Wang, 1991). Both Eqs. (12) and (13) are transformed into equivalent sets of polynomial equations with triangular structure, leaving all the coefficients of the variables as formal (symbolic) parameters instead of numerical values. In such a way, the solutions

obtained generally hold for the whole class of link systems. Therefore, they are computed just once, in a preliminary phase, and then specialized at each iteration.

Some detailed examples of solutions obtained by means of the Gröbner basis method can be found in the works of Cox et al. (1992) and Lazard (1992). The method is briefly described in Appendix A.

Since all the symbolic solutions of Eqs. (13) and (12) are available, either Eqs. (14) and (15) or the *a posteriori* criterion can be applied in order to identify the configuration $C_{\mathrm{r}}^{(k)}$. Moreover, all the possible starting rigid configurations can be determined from the symbolic solutions of Eq. (13).

5. Convergence analysis

The convergence analysis of the proposed algorithm is not trivial because of the nonlinearity of the compensation step. Moreover, the recursive equation of the iteration scheme can not be generally expressed in a closed or analytical form. As a consequence, in order to determine only sufficient but not necessary conditions for the algorithm to converge, the analysis has been performed by linearizing the compensation step.

At the typical step k, the compatibility equations are identically satisfied due to the choice of $\mathbf{P}_{\mathrm{r}}^{(k)}$. Linearizing the compatibility equation in the neighborhood of the operating point $(\mathbf{q}_{\mathrm{d}}^{(k)}, \mathbf{P}^{(k)}, \mathbf{g}_{\mathrm{d}}^{(k)})$ which describes the configuration $C_{\mathrm{d}}^{(k)}$ of $S_{\mathrm{r}}^{(k)}$:

$$\mathbf{J}_q\left(\mathbf{q}_{\mathrm{d}}^{(k)}, \mathbf{P}^{(k)}, \mathbf{g}_{\mathrm{d}}^{(k)}\right)\left(\mathbf{q}-\mathbf{q}_{\mathrm{d}}^{(k)}\right)+\mathbf{J}_P\left(\mathbf{q}_{\mathrm{d}}^{(k)}, \mathbf{P}^{(k)}, \mathbf{g}_{\mathrm{d}}^{(k)}\right)\left(\mathbf{P}_{\mathrm{r}}-\mathbf{P}^{(k)}\right)=\mathbf{0},$$

the correction for compensating the positioning error can be expressed as

$$\mathbf{q}^{(k+1)}-\mathbf{q}^{(k)}=-\mathbf{J}_q^{-1}\left(\mathbf{q}_{\mathrm{d}}^{(k)}, \mathbf{P}^{(k)}, \mathbf{g}_{\mathrm{d}}^{(k)}\right)\mathbf{J}_P\left(\mathbf{q}_{\mathrm{d}}^{(k)}, \mathbf{P}^{(k)}, \mathbf{g}_{\mathrm{d}}^{(k)}\right)(\bar{\mathbf{P}}-\mathbf{P}^{(k)}). \tag{16}$$

The right hand side of Eq. (16) is the leading term of the nonlinear correction at the typical step k. Thus, the main iteration formula can be written as

$$\mathbf{q}^{(k+1)}=\mathbf{q}^{(k)}-\mathbf{A}_{\mathrm{d}}^{-1}\mathbf{F}(\mathbf{q}^{(k)}),$$

where

$$\mathbf{F}(\mathbf{q}^{(k)})=\bar{\mathbf{P}}-\mathbf{P}_{\mathrm{r}}(\mathbf{q}^{(k)})-\mathbf{u}\left(\mathbf{q}^{(k)}, \mathbf{P}_{\mathrm{r}}(\mathbf{q}^{(k)})\right).$$

The term $\mathbf{P}_{\mathrm{r}}(\mathbf{q}^{(k)})$ denotes only a functional dependence and not necessarily an analytical one. As can be seen from Eq. (16), the iteration matrix is taken as

$$\mathbf{A}_{\mathrm{d}}^{(k)}=\left.\frac{\partial \mathbf{P}_{\mathrm{r}}}{\partial \mathbf{q}}\right|_{S_{\mathrm{r}}^{(k)}}=\mathbf{J}_P^{-1}\left(\mathbf{q}_{\mathrm{d}}^{(k)}, \mathbf{P}^{(k)}, \mathbf{g}_{\mathrm{d}}^{(k)}\right)\mathbf{J}_q\left(\mathbf{q}_{\mathrm{d}}^{(k)}, \mathbf{P}^{(k)}, \mathbf{g}_{\mathrm{d}}^{(k)}\right).$$

Hence, the local condition for the algorithm to converge is

$$\rho\left(\mathbf{I}-\left[\mathbf{J}_q^{-1}\mathbf{J}_P\right]\Big|_{C_{\mathrm{d}}}\left[\mathbf{J}_P^{-1}\mathbf{J}_q-\mathbf{U}_q-\mathbf{U}_P\mathbf{J}_P^{-1}\mathbf{J}_q\right]\Big|_{C_{\mathrm{r}}}\right)<1. \tag{17}$$

Under the assumption that the displacements are sufficiently small to neglect the distinction between the deformed and the undeformed configurations, from Eq. (17) it follows that

$$\rho\left(\mathbf{J}_q^{-1}\mathbf{J}_P\left(\mathbf{U}_q - \mathbf{U}_P\mathbf{J}_P^{-1}\mathbf{J}_q\right)\right) < 1. \tag{18}$$

If the change of the displacement field with respect to the change of the undeformed configuration is small, i.e.

$$\rho(\mathbf{U}_q) \ll 1,$$

$$\rho(\mathbf{U}_P) \ll 1$$

and if the matrices $\mathbf{J}_q^{-1}$ and $\mathbf{J}_P^{-1}$ both exist, the local condition (18) is always satisfied. Moreover, under the assumption of small displacements the initial configuration, which is taken as a solution of the inverse kinematics problem of the equivalent rigid link system, is sufficiently accurate to guarantee a global convergence. However, as can be seen from the numerical examples, the hypotheses assumed to prove the convergence of the algorithm are too restrictive and Eq. (18) is a sufficient but not a necessary condition.

6. Numerical examples

In this section, some numerical tests are presented to assess advantages and drawbacks of the outlined method in comparison with the other schemes proposed in the literature.

6.1. Example 1 — Planar three degrees of freedom serial link system: ESA–SMS space manipulator (Svinin and Uchiyama, 1994)

The first example deals with a planar three-link system, shown in Fig. 6 and quoted in Svinin and Uchiyama (1994). Its model parameters are chosen to be in correspondence with those of ESA–SMS space manipulator (Svinin and Uchiyama, 1994). The link system consists of two flexible (link 1 and link 2) and one undeformable (link 3 or end-effector) members mutually connected by revolute joints. The first two links of the manipulator are modeled as identical elastic homogenous cylindrical straight beams, with length $l_1 = 3$ m and $l_2 = 3$ m, respectively. The cross sectional moment of inertia about the bending axis and Young's modulus of elasticity are taken as $I_\alpha = 0.7363 \times 10^{-4}\,\mathrm{m}^4$ and

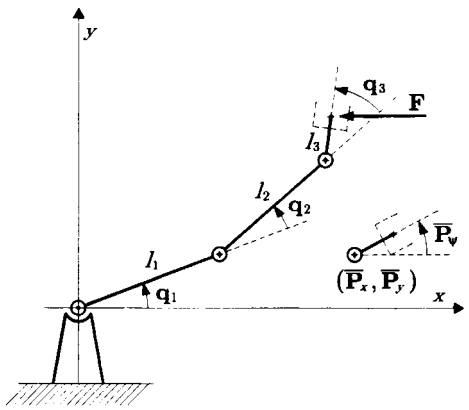

Fig. 6. Planar three link system: ESA–SMS space manipulator.

$E = 1.2223 \times 10^9$ N/m^2, respectively. The third link is modeled as an undeformable beam of length $l_3 = 0.5$ m.

According to Fig. 6, the vector of the joint degrees of freedom is $\mathbf{q}^T = [\mathbf{q}_1\ \mathbf{q}_2\ \mathbf{q}_3]$, where $\mathbf{q}_i$ is the counterclockwise angle from link $i-1$ to link i and the vector $\mathbf{g}$ is taken as $\mathbf{g}^T = [l_1\ l_2\ l_3]$. The end-effector position is completely determined by the position of the third joint, $(\bar{\mathbf{P}}_x, \bar{\mathbf{P}}_y)$, and the orientation of the third link, $\bar{\mathbf{P}}_\psi$, thus $\bar{\mathbf{P}}^T = [\bar{\mathbf{P}}_x\ \bar{\mathbf{P}}_y\ \bar{\mathbf{P}}_\psi]$. The tip of the end-effector is subjected to a horizontal concentrated force $\mathbf{F}$. The finite element method is used to solve the elastic equilibrium problem of the link system.

The global corrections of the joint degrees of freedom with respect to the initial rigid configuration (i.e. with respect to the solution of the inverse kinematics problem of the rigid link system) are denoted by $\Delta\mathbf{q}_i$ and are plotted versus the target position in the graphs of Fig. 7. The target position is varied whilst maintaining a constant x coordinate $\bar{\mathbf{P}}_x$ and the orientation $\bar{\mathbf{P}}_\psi$, and adapting only the y coordinate $\bar{\mathbf{P}}_y$. Different curves in each graph refer to different load values.

Fig. 8 shows the variation of the end-effector positioning error with respect to the number of iterations, for two given target positions. These graphs evidence the good performance of the outlined method.

The performances of the proposed method (*RNC*) with respect to the Newton–Raphson method (*NR*) and the linear compensation schemes (*RCL* and *DCL*) are compared in Table 1. For the sake of comparison, the same starting point is assumed for all the algorithms and it coincides with a rigid body motion solution obtained from the Gröbner basis method. The number of iterations for the algorithms to converge for two values of the force is checked in the course of three tests and summarized in Table

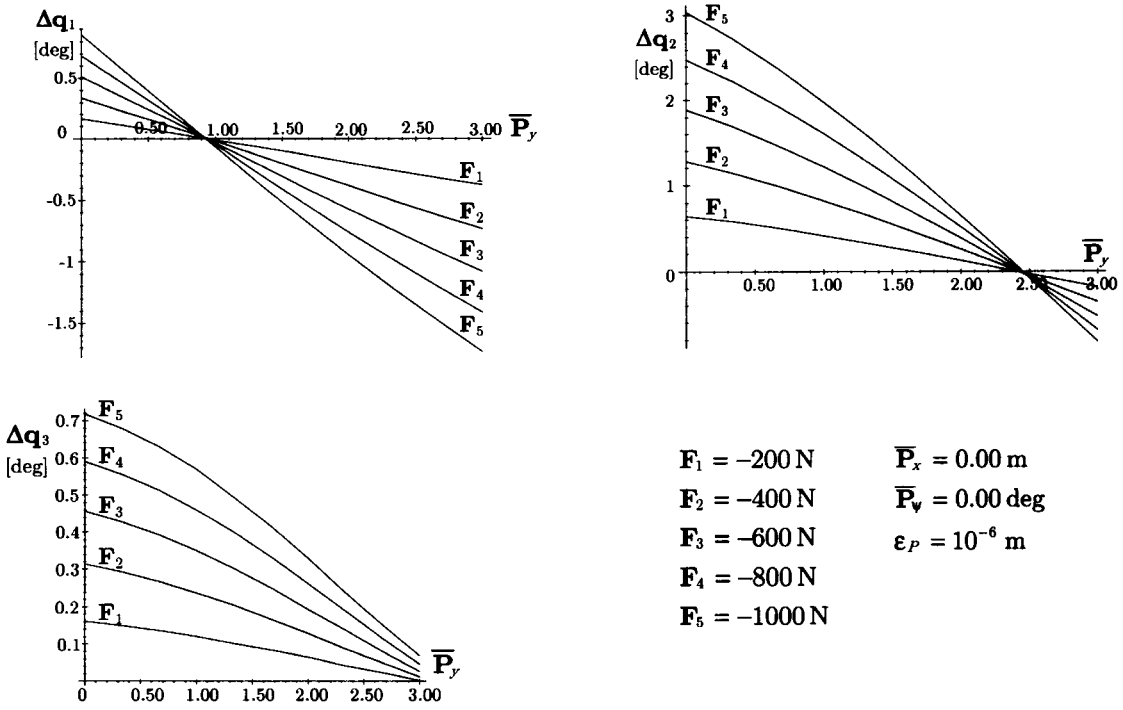

Fig. 7. Global corrections of the joint degrees of freedom with respect to the initial rigid configuration.

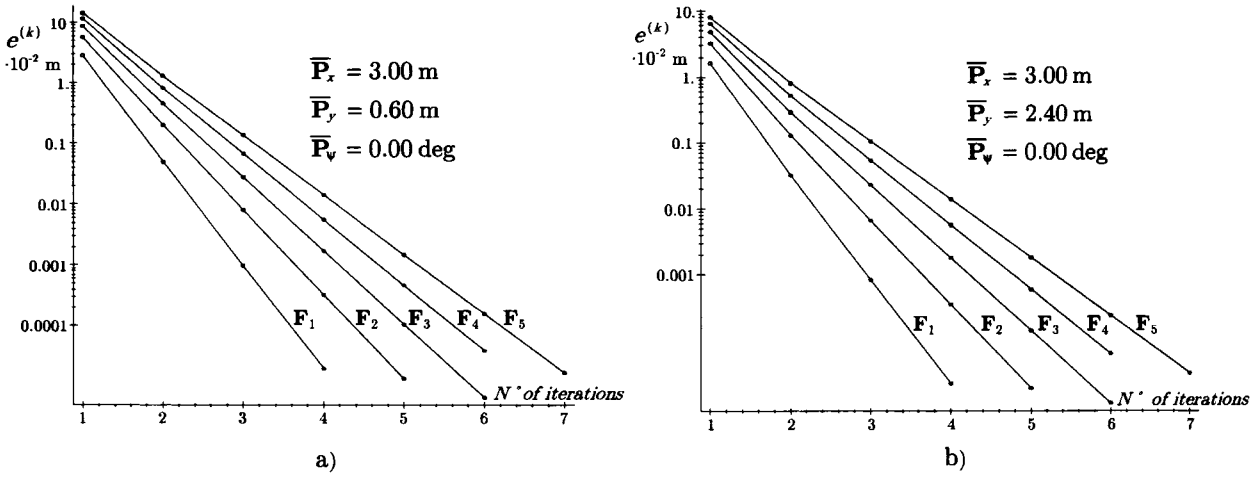

Fig. 8. End-effector positioning error versus the number of iterations for two given target positions.

1. The prescribed tolerance for the end-effector position is taken as $\varepsilon_p = 10^{-6}$ m. Furthermore, for each test, the residual error of the *DLC* algorithm,

$$e_r = \|\hat{\mathbf{P}} - \bar{\mathbf{P}}\|_W,$$

between the obtained solution, $\hat{\mathbf{P}}$, and the prescribed target position, is collected in Table 2. Referring to three different cases, the error $e^{(k)}$ against the number of iterations is shown in Fig. 9.

Some considerations can be drawn from the analysis of the exposed results.

It is necessary to distinguish the cases where the target position is close to a kinematic singularity from the others. The end-effector positions corresponding to the kinematic singularities of the present link system are:

$$\mathbf{P} = (0,\ 0,\ \alpha) \text{ for } 0 \le \alpha < 2\pi,$$

$$\mathbf{P} = (\alpha,\ 0,\ \beta) \text{ for } 0 \le \alpha < 2\pi \text{ and } 0 \le \beta < 2\pi.$$

Therefore, for target positions sufficiently far from the singularities, the *NR* method exhibits the best performance, whereas the others are substantially comparable.

Getting closer to a kinematic singularity, the performance of *RLC* and *DLC* drastically decreases, being not always effective in obtaining the solution. Observing Fig. 9(a), the *NR* scheme could also be less effective than the proposed method. In fact, its iteration matrix can become singular or quasi-singular depending on the target position and the load value.

The results shown in Table 2 confirm that the *DLC* method does not converge to a solution of the problem, and the residual error is not always acceptable for the purpose of the analysis.

Notice that, in all the tests performed, *NR*, *RLC* and *DLC* are started with an accurate estimation of the solution, which corresponds to a rigid configuration compatible with the target position. Moreover, at most one solution for each test is obtained. On the other hand, the proposed algorithm is self-starting

Table 1
Comparison between the proposed algorithm and other references. Prescribed accuracy: $\varepsilon_p = 10^{-6}$ m

Test 1a	$\mathbf{F} = -500$ N, $\bar{\mathbf{P}}_x = 3.00$ m										
$\bar{\mathbf{P}}_y$	0.00	0.30	0.60	0.90	1.20	1.50	1.80	2.10	2.40	2.70	3.00
NR	3	3	3	3	3	3	3	3	3	3	3
RLC	5	5	5	5	5	5	4	5	5	5	5
DLC	4	4	5	5	5	5	4	4	5	5	5
RNC	5	5	5	5	5	5	4	5	5	6	6
Test 1b	$\mathbf{F} = -1000$ N, $\bar{\mathbf{P}}_x = 3.00$ m										
$\bar{\mathbf{P}}_y$	0.00	0.30	0.60	0.90	1.20	1.50	1.80	2.10	2.40	2.70	3.00
NR	4	4	4	4	3	3	3	3	3	3	4
RLC	6	6	6	6	6	6	6	6	7	7	7
DLC	5	5	6	6	6	6	5	6	6	6	6
RNC	6	7	7	7	7	7	6	7	7	7	7
Test 2a	$\mathbf{F} = -500$ N, $\bar{\mathbf{P}}_x = 0.10$ m										
$\bar{\mathbf{P}}_y$	0.00	0.05	0.10	0.15	0.20	0.25	0.30	0.35	0.40	0.45	0.50
NR	$\propto$	4	4	3	3	3	3	3	3	3	3
RLC	13	11	8	6	5	5	4	4	4	4	4
DLC	16	13	9	7	6	4	4	4	4	4	4
RNC	4	5	5	5	5	5	5	4	4	4	4
Test 2b	$\mathbf{F} = -1000$ N, $\bar{\mathbf{P}}_x = 0.10$ m										
$\bar{\mathbf{P}}_y$	0.00	0.05	0.10	0.15	0.20	0.25	0.30	0.35	0.40	0.45	0.50
NR	5	5	5	4	3	3	3	3	3	3	3
RLC	22	17	12	9	7	6	5	5	5	5	6
DLC	25	19	13	9	7	5	5	5	5	4	5
RNC	6	8	8	7	7	7	6	6	5	5	6
Test 3a	$\mathbf{F} = -500$ N, $\bar{\mathbf{P}}_x = -0.10$ m										
$\bar{\mathbf{P}}_y$	0.00	0.05	0.10	0.15	0.20	0.25	0.30	0.35	0.40	0.45	0.50
NR	3	3	3	3	3	3	3	3	3	3	3
RLC	$\propto$	$\propto$	70	9	6	5	4	4	4	4	4
DLC	$\propto$	$\propto$	92	11	7	5	4	4	4	4	4
RNC	3	3	4	5	5	5	5	4	4	4	4
Test 3b	$\mathbf{F} = -1000$ N, $\bar{\mathbf{P}}_x = -0.10$ m										
$\bar{\mathbf{P}}_y$	0.00	0.05	0.10	0.15	0.20	0.25	0.30	0.35	0.40	0.45	0.50
NR	4	4	4	4	4	3	3	3	3	3	3
RLC	$\propto$	$\propto$	$\propto$	$\propto$	13	7	6	5	5	5	6
DLC	$\propto$	$\propto$	$\propto$	$\propto$	15	7	5	5	5	4	5
RNC	4	5	5	5	6	6	6	5	4	5	6

Table 2
Residual end-effector positioning error of the *DLC* algorithm

$\bar{\mathbf{P}}_y$	0.00	0.30	0.60	0.90	1.20	1.50	1.80	2.10	2.40	2.70	3.00
$\bar{\mathbf{P}}_x = 3.00$	1.93	1.45	1.01	0.62	0.30	0.09	0.07	0.14	0.27	0.57	1.04

$\bar{\mathbf{P}}_y$	0.00	0.05	0.10	0.15	0.20	0.25	0.30	0.35	0.40	0.45	0.50
$\bar{\mathbf{P}}_x = 0.10$	2.49	1.03	0.28	0.04	0.03	0.06	0.07	0.06	0.06	0.05	0.04
$\bar{\mathbf{P}}_x = -0.10$	/	/	0.16	0.04	0.03	0.06	0.07	0.06	0.06	0.05	0.04

$e_r \times 10^{-2}$ m, $\mathbf{F} = -500$ N

$\bar{\mathbf{P}}_y$	0.00	0.30	0.60	0.90	1.20	1.50	1.80	2.10	2.40	2.70	3.00
$\bar{\mathbf{P}}_x = 3.00$	7.72	5.83	4.05	2.48	1.21	0.35	0.30	0.53	1.10	2.31	4.19

$\bar{\mathbf{P}}_y$	0.00	0.05	0.10	0.15	0.20	0.25	0.30	0.35	0.40	0.45	0.50
$\bar{\mathbf{P}}_x = 0.10$	9.70	3.85	1.04	0.15	0.15	0.24	0.27	0.26	0.23	0.20	0.15
$\bar{\mathbf{P}}_x = -0.10$	/	/	/	/	0.17	0.24	0.27	0.26	0.23	0.20	0.15

$e_r \times 10^{-2}$ m, $\mathbf{F} = -1000$ N

and it offers all the solutions of the problem, even if, for the sake of brevity, only one solution for each test has been shown.

As can be observed from the exposed results, *RNC* is the only scheme which is always effective in getting the solutions, resulting in being unaffected by the kinematic singularities.

6.2. Example 2 — Planar three degrees of freedom hybrid link system

The second example deals with a planar hybrid link system shown in Fig. 10, which is made up of two subsystems mutually connected. The lower module is a one degree of freedom parallel system, which comprises one undeformable element (link 3) supported at both end by two flexible members (link 1 and link 2). Link 1 is assumed to be a prismatic joint, i.e. its length can be varied starting from the reference length l_1. The upper module is a two degrees of freedom serial link system, which consists of one flexible (link 4) and one undeformable (link 5 or end-effector) member.

All the links of the whole system are mutually connected through revolute joints, link 1 is hinged and link 2 is fixed to the ground. The flexible members are assumed to be straight beams with the same geometrical and elastic properties of the links of example 1. According to Fig. 10, the lengths of the links are $l_1 = 3$ m, $l_2 = 3$ m, $l_3 = 3$ m, $l_4 = 1.5$ m and $l_5 = 0.5$ m, respectively, and the vector $\mathbf{g}$ is taken as $\mathbf{g}^T = [l_0\ l_2\ l_3\ l_4\ l_5\ \vartheta_2]$, where $l_0 = 6$ m and $\vartheta_2 = 2\pi/3$. The vector of the joint degrees of freedom is $\mathbf{q}^T = [\mathbf{q}_1\ \mathbf{q}_2\ \mathbf{q}_3]$, where $\mathbf{q}_1$ is the elongation (i.e. the difference between the current and the reference length) of link 1 and $\mathbf{q}_2$ and $\mathbf{q}_3$ are the counterclockwise angle from link 3 to link 4 and link 4 to link 5, respectively. The load, $\mathbf{F}^T = [\mathbf{F}_x\ \mathbf{F}_y]$, is applied at the free extremity of the end-effector. Analogously to example 1, the

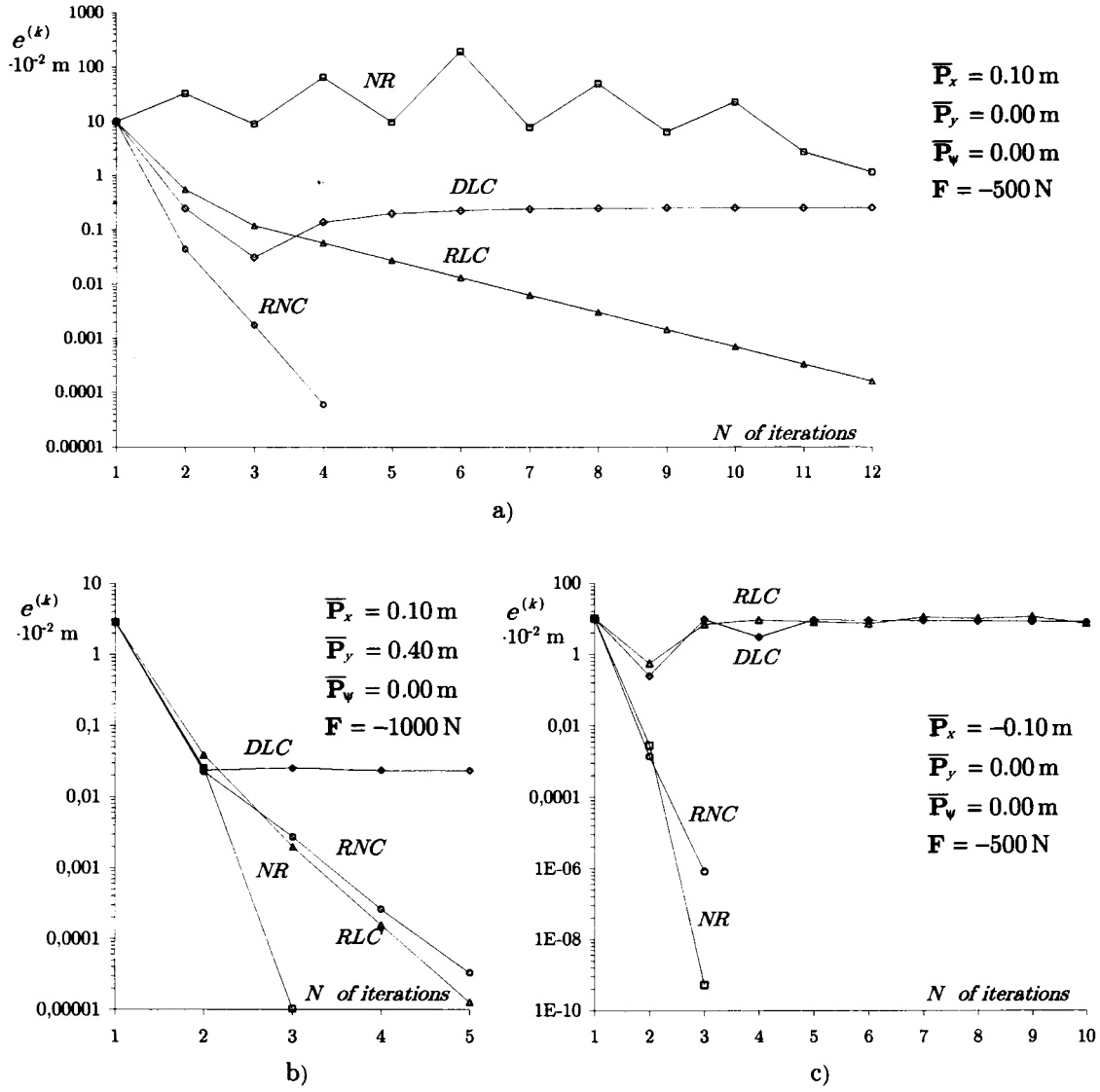

Fig. 9. Comparison between the proposed algorithm and other references.

end-effector position is given by $\bar{\mathbf{P}}^{\mathrm{T}} = [\bar{P}_x\ \bar{P}_y\ \bar{P}_\psi]$, and the elastic equilibrium problem is solved at each step by means of the finite element method.

Numerical tests for several target positions and load values have been performed, comparing the proposed algorithm with the *RLC* scheme. No comparisons have been made with the *DLC* scheme, since it is not applicable to hybrid systems, and with the *NR* scheme, because of the complexity of its implementation and the cumbersome computations involved. In practice, the *NR* algorithm is not applicable even in such a simple case.

Both the direct and the inverse kinematics problems generally admit two solutions. Eqs. (14) and (15) have been adopted in order to update the system configuration and they have been effective in all the

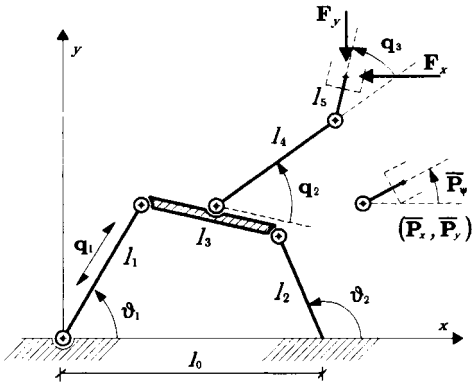

Fig. 10. Planar three degrees of freedom hybrid link system.

numerical tests. For the sake of comparison, the *RLC* scheme has been always started up with the solutions of the inverse problem of the equivalent rigid system.

Fig. 11 depicts the error $e^{(k)}$ versus the number of iterations for three different target positions. For each test both the solutions compatible with the prescribed end-effector position are shown, even if they refer to different values of the applied force.

When link 4 is aligned to link 3, $\mathbf{q}_2 = 0$, the link system locally loses a degree of freedom and the related configurations correspond to kinematic singularities.

As emerges from tests 1 and 3, if the target position is sufficiently far from the kinematic singularities the proposed algorithm and the *RLC* scheme exhibit comparable performances. This circumstance is due to the accurate initial configurations employed to start up the *RLC* scheme. Failing good initial approximations of the solution, the performance of the *RLC* algorithm gets worse, becoming sensibly inferior with respect to the *RNC* algorithm.

On the other hand, as it emerges from test 2, if the target position gets closer to a kinematic singularity, the *RLC* scheme can fail to converge, while the proposed method is still effective, even if its rate of convergence becomes slower.

The results are in agreement with those exposed in Example 1, confirming the general applicability of the present method and its better performance with respect to the other schemes.

7. Conclusions

A method for a systematic approach to the inverse kinematics problem of flexible link systems has been presented in this paper. The resulting algorithm is based upon a nonlinear compensation scheme, which makes use of the Gröbner basis method. At the current state of the art, the applicability of the outlined procedure is partially confined due to the practical limitations of the existing implementations of the Gröbner basis method (e.g. Char et al., 1991; Gräbe, 1993). On the other hand, some numerical tests performed on different system typologies result in a better performance of the present method with respect to the methods which apply linear compensation schemes. In fact, the proposed algorithm is not affected by the kinematic singularities, it is self-starting and it permits to get all the solutions of the problem.

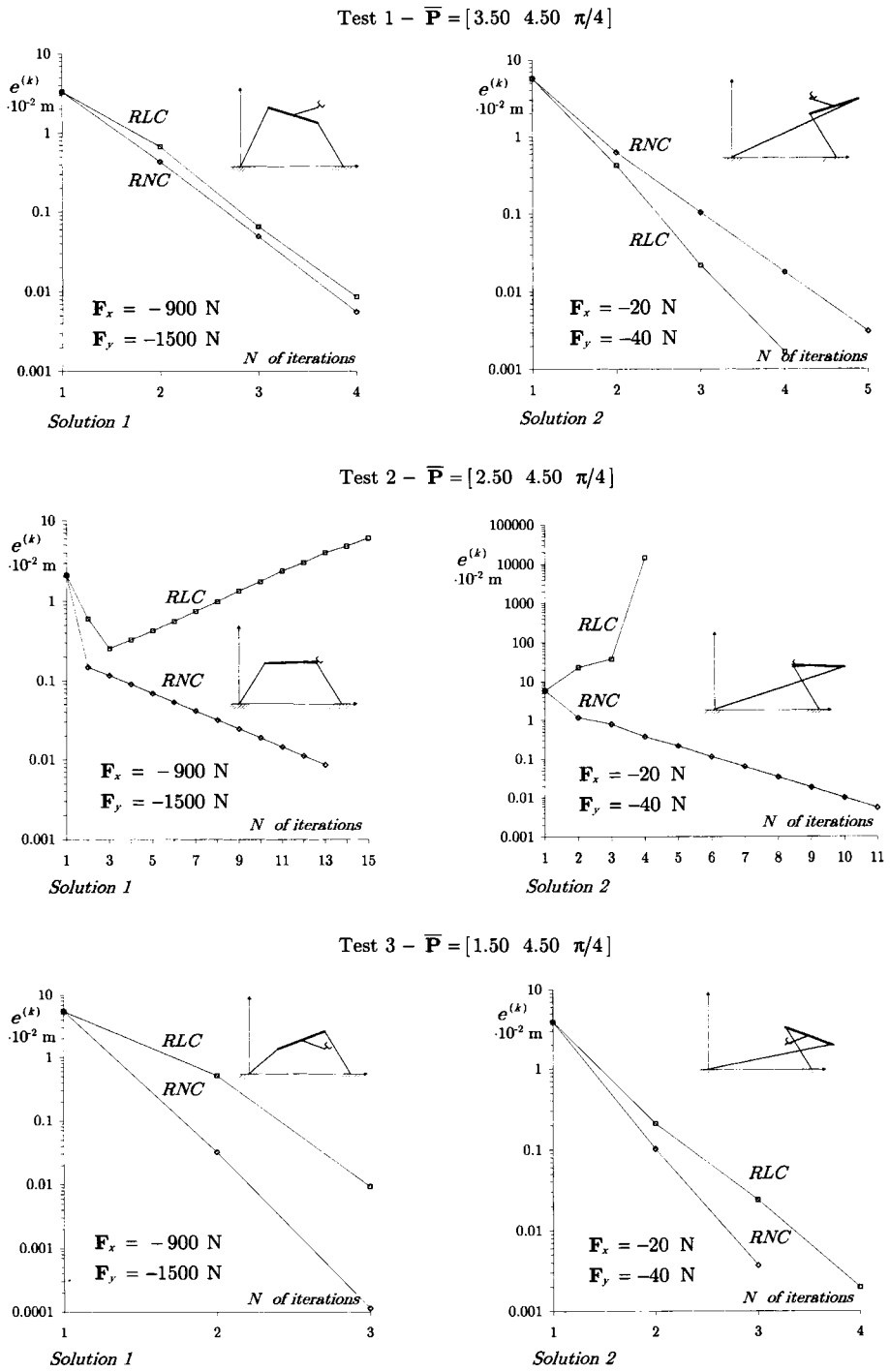

Fig. 11. Comparison between the proposed algorithm and the *RLC* scheme.

Acknowledgements

The author expresses a grateful acknowledgement to Prof. M. Manaresi, Università di Bologna, Italy. The financial support of the (Italian) Ministry for University and Scientific Research (MURST) made this work possible. Numerical developments were performed at Laboratorio di Meccanica Computazionale (LAMC), DISTART, Università di Bologna, Italy.

Appendix A

The Gröbner basis method is applied in the compensation step to obtain the implicit symbolic solutions of Eqs. (12) and (13). In the following, the method is only briefly described, but more details and some examples can be found in the works of Cox et al. (1992) and Lazard (1992).

Firstly, both the systems to be solved are converted into equivalent polynomial systems in suitable variables, $\mathbf{x}$, through the parametrization of the unit circle (Cox et al., 1992). Then, a Gröbner basis of the ideal generated by each set of polynomials is computed with respect to the pure lexicographic order, in the ring $\mathbb{R}(\boldsymbol{\beta})[\mathbf{x}]$ — $\boldsymbol{\beta}$ denotes the symbolic vector which parameterizes the set of polynomials. In particular, the resolutions of the inverse and the direct problem are carried out by setting $\boldsymbol{\beta}^{\mathrm{T}}=[\mathbf{g}\ \mathbf{P}]$ and $\boldsymbol{\beta}^{\mathrm{T}}=[\mathbf{g}\ \mathbf{q}]$, respectively.

The systems of polynomial equations, obtained by equating the computed Gröbner bases to zero, are proved to have a triangular structure and to be equivalent to the initial sets of equations, for each (numerical) value of $\boldsymbol{\beta}$, which does not nullify any leading coefficient of the bases. Therefore, at the typical step, each implicit symbolic solution is opportunely specialized and the resulting sequence of polynomial equations, in only one variable, is numerically solved. In general, just one of these equations is of high degree.

References

Baillieul, J., Martin, D.P., 1990. Resolution of kinematic redundancy. Robotics, Proceedings of Symposia in Applied Mathematics 41, 49–89.

Boudreau, R., Tukkan, N., 1996. Solving the forward kinematics of parallel manipulators with a genetic algorithm. Journal of Robotic Systems 13, 111–125.

Buchberger, B., 1985. Gröbner bases: An algorithmic method in polynomial ideal theory. In: Bose, N.K. (Ed.), Multidimensional System Theory. D. Reidel Publishing Co, pp. 184–232.

Canny, J., 1988. The Complexity of Robot Motion Planning. MIT Press, Cambridge.

Chang, L.-W., Hamilton, J.F., 1991. The kinematics of robotic manipulators with flexible links using an Equivalent Rigid Link System (ERLS) model. Transactions of the ASME, Journal of Dynamic System, Measurement, and Control 113, 48–53.

Char, B.W., Geddes, K.O., Gonnet, G.H., Leong, B.L., Monagan, M.B., Watt, S.M., 1991. Maple V Language Reference Manual. Springer–Verlag, New York.

Colbaugh, R., Glass, K., Seraji, H., 1990. An adaptive inverse kinematics algorithm for robot manipulators. In: Proceedings of American Control Conference, vol. 3, pp. 2281–2286.

Cox, D., Little, J., O'Shea, D., 1992. In: Ideals, Varieties, and Algorithms: an Introduction to Computational Algebraic Geometry and Commutative Algebra. Springer–Verlag, New York (pp. 48–112 and 253–305).

Denavit, J., Hartenberg, R.S., 1955. A kinematics notation for lower-pair mechanisms based on matrices. Transactions of the ASME, Journal of Applied Mechanics 77, 215–221.

Derby, S., 1983. The deflection and compensation of general purpose robot arms. Mechanism and Machine Theory 18, 445–450.

Fu, K.S., Gonzalez, R.C., Lee, C.S.G., 1987. Robotics: Control, Sensing, Vision, and Intelligence. McGraw–Hill, New York.

Gosselin, C.M., Perreault, L., Vaillancourt, C., 1995. Simulation and computer aided kinematic design of three degree of freedom spherical parallel manipulators. Journal of Robotic Systems 12, 857–869.

Gräbe, H.-G., 1993. *Cali* — A Reduce Package for Commutative Algebra (Available through the Reduce library, e.g. at redlib@rand.org).

Innocenti, C., 1995. Analytical form direct kinematics for the second scheme of 5–5 general geometry fully parallel manipulator. Journal of Robotic Systems 2, 661–676.

Koren, Y., 1987. Robotics for Engineers. McGraw–Hill, New York.

Lazard, D., 1992. Stewart platforms and Gröbner basis. In: 3rd International Workshop on Advances in Robot Kinematic (3ARK), Ferrara, Italy, September 7–9, pp. 136–142.

Lazard, D., Merlet, J.P., 1994. The (true) Stewart platform has 12 configurations. In: IEEE Proceedings of the International Conference on Robotics and Automation, San Diego, California, May 8–13, pp. 2160–2165.

Lee, E.H., Liang, C., 1988. Displacement analysis of the general spatial 7-link 7R mechanisms. Mechanism and machine theory 23, 219–226.

Lin, P.P., Chiang, H.D., Cui, X.X., 1991. An improved method for on-line calculation and compensation of the static deflection of a robot end-effector. Journal of Robotic Systems 8, 267–288.

Lopez, M.J., Recio, T., 1993. The Romin inverse geometric model and the dynamic evaluation method. In: Computer Algebra in Industry. John Wiley & Sons, West Sussex.

Mavroidis, C., Ouezdou, F.B., Bidaud, P., 1994. Inverse kinematics of six-degree of freedom general and special manipulators using symbolic computation. Robotica 12, 421–430.

Ortega, J.M., Rheinboldt, W.C., 1970. Iterative Solution of Nonlinear Equations in Several Variables. Academic Press Inc, San Diego.

Paul, R.P., 1982. Robot Manipulators: Mathematics, Programming, and Control. MIT Press, Cambridge.

Shahinpoor, M., 1992. Kinematics of a parallel serial (hybrid) manipulator. Journal of Robotic Systems 9, 17–36.

Svinin, M.M., Uchiyama, M., 1994. A new compensation scheme for the inverse kinematics tasks of flexible robot arms. In: IEEE Proceedings of the International Conference on Robotics and Automation, San Diego, California, May 8–13, pp. 315–320.

Tornambe, A., 1990. An asymptotic observer for solving the inverse kinematics problem. Proceedings of American Control Conference 2, 1774–1779.

Tsai, L.-W., Morgan, A.P., 1985. Solving the kinematics of the most general six and five degree of freedom manipulators by continuation methods. Journal of Mechanisms, Transmissions, and Automation in Design 107, 189–200.

Ubertini, F., 1996. A method of analysis for the kinematics problem of flexible link systems. In: Proceedings of the Joint Conference of Italian Group of Computational Mechanics and Ibero–Latin American Association of Computational Methods in Engineering, Padova, Italy, September 25–27, pp. 357–360.

Wang, D.M., 1991. Reasoning about geometric problems using algebraic methods. In: Proceedings Medlar 24 Month Review Workshop, Grenoble. J. Kepler University, Linz (Technical Report 91_s1.0, Risc–Linz).

Zhang, C., Song, S.M., 1992. Forward kinematics of a class of parallel (Stewart) platforms with closed form solutions. Journal of Robotic Systems 9, 93–112.